Diversity of Pacific Meridional Mode and its distinct impacts on El Niño-Southern Oscillation

Jiuwei Zhao[1], Jong-Seong Kug[2], Jae-Heung Park[3], and Soon-Il An[4]

[1]Nanjing University of Information Science and Technology
[2]POSTECH
[3]Pohang University of Science and Technology
[4]Yonsei University

November 22, 2022

Abstract

Numerous studies have demonstrated that the Pacific Meridional Mode (PMM) plays a vital role in determining El Niño-Southern Oscillation (ENSO) events in the following winter season. However, little attention has been given to significant differences among the spatial patterns of the PMM. Here we show that the PMM exhibits a large diversity in spatial patterns, leading to distinct impacts on ENSO. Based on objective clustering analysis, two distinct spatial patterns of the PMM are detected. Cluster 1 (C1) PMM exhibits a strong sea surface temperature dipole over the subtropical eastern Pacific and mid-latitude central Pacific whereas cluster 2 (C2) features a classic dipole over the subtropical eastern Pacific and equatorial cold tongue regions. We find that the C1 PMM is strongly linked to ENSO events while the C2 PMM has no statistically significant relations with following ENSO. This gives new implications for ENSO dynamics and predictions.

Diversity of Pacific Meridional Mode and its distinct impacts on El Niño-Southern Oscillation

Jiuwei Zhao[1], Jong-Seong Kug[1*], Jae-Heung Park[1] and Soon-Il An[2]

[1]Division of Environmental Science and Engineering, Pohang University of Science & Technology (POSTECH), Pohang, Korea

[2]Department of Atmospheric Sciences, Yonsei Univeristy, Seoul, Korea

*Corresponding author: Prof. Jong-Seong Kug
Division of Environmental Science and Engineering (DESE),
Pohang University of Science and Technology (POSTECH), Korea.
Email: jskug1@gmail.com

Key points:

- The Pacific Meridional Mode has strong spatial diversity that can be separated into two groups
- These two types of the spring PMM have distinct impacts on ENSO events in the following winter
- We suggest an optimal pattern of the spring PMM for ENSO prediction

Abstract

Numerous studies have demonstrated that the Pacific Meridional Mode (PMM) plays a vital role in determining El Niño-Southern Oscillation (ENSO) events in the following winter season. However, little attention has been given to significant differences among the spatial patterns of the PMM. Here we show that the PMM exhibits a large diversity in spatial patterns, leading to distinct impacts on ENSO. Based on objective clustering analysis, two distinct spatial patterns of PMM are detected. Cluster 1 (C1) PMM exhibits a strong sea surface temperature dipole over the subtropical eastern Pacific and mid-latitude central Pacific whereas cluster 2 (C2) features a dipole over the subtropical eastern Pacific and equatorial cold tongue region. We find that the C1 PMM is strongly linked to ENSO events while the C2 PMM has no statistically significant relations with following ENSO. This gives new implications for ENSO dynamics and predictions.

Key words: PMM diversity, cluster, ENSO

1 Introduction

The North Pacific Meridional Mode (PMM) is characterized by an anomalous meridional sea surface temperature (SST) gradient coupled with anomalous winds from a cold to warm flank over the eastern North Pacific (ENP; Amaya, 2019; Chiang & Vimont, 2004; Vimont et al., 2003). Previous studies (Chang et al., 2007; Yu & Kim, 2011) have summarized that spring PMM events can trigger the following El Niño-Southern Oscillation (ENSO); the PMM is thus considered a crucial precursor for the prediction of ENSO events.

Numerous works have focused on the origin of the PMM and its impact on ENSO, as well as understanding the interactions between them. A branch of the PMM SST warming off coastal California in spring can enhance subtropical convection over the ENP, which can in turn induce westerly anomalies. Wind anomalies associated with this region are further attributed to the warming and southwestward extension of SSTs in the following seasons *via* the wind-evaporation-SST (WES) mechanism (Xie & Philander, 1994) and thereby trigger El Niño events through positive feedbacks over the equatorial Pacific. A seasonal foot-printing mechanism (SFM) was proposed by Vimont et al. (2001, 2003) to explain the potential influence of the North Pacific Oscillation (NPO; Rogers, 1981) on ENSO events. The NPO can induce anomalous SSTs over the subtropical North Pacific by affecting latent heat fluxes. Previous studies (Kao & Yu, 2009; Yu et al., 2010) have argued that SST anomalies induced by the SFM resemble the pattern of the PMM SST. These two extratropical SST patterns have therefore been treated as key players in linking the extratropical Pacific to ENSO.

More recently, PMM has also been considered as a crucial factor to induce ENSO diversity (Yu et al., 2010, 2017; Yang et al., 2018). Stuecker (2018) found that the PMM and central Pacific (CP) ENSO can excite mutually, implying a positive feedback between these two phenomena. Yu & Fang (2018) recently proposed that the SFM could significantly contribute to central Paicific ENSO events while the charge–discharge mechanism has a greater influence on conventional ENSO events. The SFM contributes to SST anomalies over the subtropical ENP while the charge–discharge mechanism modulates SST anomalies over the cold tongue (CT) region, where the SST anomalies of the PMM show significant varibility. The connection between these anomalies and both conventional and CP ENSO events also implies spatial differences in anomalous PMM SST patterns.

Although previous studies have documented possible physical processes of the PMM in exciting ENSO events, it has been seldom discussed how efficiently the PMM can induce ENSO events. Park et al. (2013) showed that only 5 positive events among 12 were linked to El Niño events in the following year and argued that the spatial pattern of the NPO might be a critical parameter for controlling the evolution of ENSO. We noted from their study that the PMM patterns shown are visibly different between the two groups. As shown in Figure 1a, we found that approximately 40% (13) of all PMM events (33) are strongly related to ENSO events. By further tracking these two groups of PMM events, we found that the main differences were concentrated on their anomalous SST patterns (Fig. 1d and 1f), which may lead to different roles in inducing ENSO events. Previous studies have shown the ubiquity of diversity in ENSO (Ashok et al., 2007; Kug et al., 2009; Yeh et al., 2009; Wang et al. 2019a) and the Madden Julian Oscillation (Wang et al. 2019b). The PMM could also exhibit diversity in its spatial patterns, which would further result in distinct behavior affecting the ENSO events.

Here, we propose a method to objectively delineate the diversity of the PMM and its impact on ENSO events. The reanalysis datasets and clustering method used to classify PMM events in this study are introduced in Section 2. The diversity of PMM and its impacts on ENSO are described in Section 3. A brief summary and discussion is presented in Section 4.

2 Data and Methodology

Extended Reconstructed SST version 5 (ERSST.v5; Huang et al., 2017) data were downloaded from the National Oceanic and Atmospheric Administration with a horizontal resolution of 2° for the 1951-2018 period. Atmospheric circulation data with a $2.5^{\circ} \times 2.5^{\circ}$ horizontal resolution, including sea level pressure (SLP) and winds at 850 hPa for the same period were downloaded from National Centers for Environmental Prediction/National Centers for Atmospheric Research reanalysis version I (NCEP/NCAR V1; Kalnay et al., 1996).

The raw PMM was download from the University of Wisconsin-Madison (http://www.aos.wisc.edu/~dvimont/MModes/RealTime/PMM.RAW.txt), which contains both interannual and interdecadal variabilities (Liu et al., 2019). A fast Fourier transform method is used to filter out decadal variability (> 10 years) from both the reanalysis data and the PMM index. We confirmed that the results of the cluster analysis were not significantly changed when applied to non-filtered data. To exclude the impact of previous ENSO events on the spring (February-May averaged; FMAM) PMM event, we linearly removed the previous November-December-January (NDJ) ENSO (Nino3.4; 5ºS-5ºN, 120ºW-170ºW) signal from the PMM time series as in Ashok et al. (2007). We also tested the removal of simultaneous ENSO signals, finding that the result was consistent (Fig. S1).

An objective K-Means clustering method (Wang et al., 2019a, b; Wilks, 2011) was used to classify diverse PMM patterns. Firstly, we linearly removed the previous NDJ Nino3.4 signal from FMAM SSTs. Secondly, 33 PMM events were selected based on a criterion of ± 0.7 standard deviation of the filtered FMAM PMM index and all negative PMM events were transformed to positive ones such that we were not required to separate positive and negative PMM events into two groups, allowing us instead to focus on pattern diversity. Thirdly, SSTs over a fixed domain (20ºS-40ºN, 150ºE-60ºW) were selected and fed into a clustering model using squared Euclidean distance to measure the similarity between each cluster member and the corresponding cluster centroid. The silhouette criterion, whose value varies from -1 to 1, was utilized to assess the skill of cluster analysis. A high silhouette value implies that the member has a high similarity with its own cluster but a lower similarity with its neighboring clusters (Kaufman & Rousseeuw, 2009).

3 Results

Previous studies have documented a statistically significant correlation between the spring PMM and the following winter ENSO index (Anderson, 2003, 2007; Larson & Kirtman, 2014). Figure 1a shows the spring PMM and the following winter Nino3.4 indices with interdecadal variability removed. The correlation is 0.28 for the period 1951-2018 and 0.45 for the period 1979-2018, both exceeding 95% confidence levels. The significant lag correlation indicates that the PMM is probably a good predictor of ENSO events. However, we evaluated 33 PMM events with amplitudes greater than 0.7 standard deviation and found that 13 cases (6 positive and 7 negative cases marked with green bars in Figure 1a) corresponded to respective ENSO events, whereas the other 20 cases (10 positive and 10 negative in red bars) were not directly related to ENSO (Fig. 1a). This indicates that some PMM events are strongly related to ENSO but others did not lead to the triggering of ENSO, implying the PMM-ENSO relationship is diverse. Furthermore, we studied composites of spring and winter SST anomalies for these 33 cases (Fig. 1b-1g). The spring PMM events show a clear tripole SST pattern with large anomalies centered over the southern CT, ENP and central North Pacific regions (Fig. 1b), but the following ENSO signal is weak (Fig. 1c).

To clarify the relationship between PMM and ENSO, we conducted a composite analysis by dividing PMM events into two groups: the first group is strongly related to ENSO events (blue bars) and the second is not (red bars; Fig. 1d-1g). An important feature shown is the significant difference in spring PMM patterns between the two groups (Fig. 1d and 1f). When the positive PMM precedes El Niño, the SST anomalies in spring show a clear dipole pattern in the northern subtropical region but insignificant negative SST anomalies over the CT region (Fig. 1d). While the PMM is not linked to ENSO development, the SST pattern shows an interhemispheric dipole over the eastern Pacific. In addition, subtropical positive SST anomalies in Figure 1d extend to the southwest as far as the equator over the CP, but negative SST anomalies are dominant over the CT region in Figure 1f, mainly over the southeastern Pacific Ocean.

Abovementioned different SST patterns suggest potential spatial diversity in the PMM, which could further lead to distinct impacts on ENSO events (Fig. 1e and 1g). To validate our hypothesis and justify the corresponding analysis, a K-Means clustering method was utilized to objectively classify 33 PMM events into 2 clusters. The composites of the PMM events for the two clusters are shown in Figure 2, with different clusters displayed in the left and right panels. Cluster 1 (C1) positive PMM events in Figure 2a are characterized by significant positive SST anomalies elongated from the CP to the subtropical ENP and negative SST anomalies over the subtropical CP region. C1 SST anomalies correspond to significant equatorial westerly anomalies in the CP and easterly anomalies in the CT regions (Fig. 2a). Similarly, negative C1 events show a strong negative SST anomaly extending from the CP to subtropical ENP, coupled with significant equatorial easterly wind anomalies in the central-western Pacific, and a positive SST anomaly in the subtropical North Pacific (Fig. 2b). However, the spatial pattern of cluster 2 (C2) PMM events (Fig. 2d and 2f) is distinct from that of C1. C2 PMM events feature a hemispheric dipole of SST anomalies over the southern tropical and northern subtropical eastern Pacific (Fig. 2d and 2f). Due to the development of strong SST anomalies over the CT region, easterly anomalies are dominant over the whole equatorial Pacific during positive phases while westerly anomalies during negative phases. These are clearly distinguished from their respective anomalous convergent and divergent patterns in C1 events (Fig. 2a and 2b).

Based on the different spatial patterns of these two types of PMM events, we refer to C1 as the western PMM (WPMM) and C2 as the eastern PMM (EPMM) events. The silhouette values of C1 and C2 PMM events are shown in Figure 2c and 2f with positive and negative PMM cases marked in red and blue, respectively. The silhouette values of C1 are, on average, higher than those of C2, indicating that the C1 shows a higher degree of "similarity" and that the spatial patterns of positive and negative WPMM events are more symmetric than the EPMM events. It is worth noting that 5 El Niño events occurred in positive WPMM years where only one event followed a positive EPMM phase. Moreover, only one La Niña event was involved in a positive WPMM phase (Fig. S2a and Table S1) and no false alarms for El Niño events were observed during our studying period, indicating that WPMM events are a better precursor for predicting ENSO events.

Table S1 gives the details of ENSO events related to the PMM. Five of the seven positive C1 events were clearly linked to the occurrence of El Niño and four of the eight negative C1 events were related to La Niña; each individual PMM case is shown in Figure S2. However, only one positive EPMM event out of the nine cases studied was followed by an El Niño event, whereas three of the nine negative EPMM events were followed by La Niña. It was also noted that the positive EPMM event followed by an El Niño case corresponded to the only negative silhouette value in C2 (Fig. 2f), meaning that this event was not a conventional EPMM event pattern. Furthermore, 2 positive EPMM and 3 negative EPMM events were even followed by La Niña and El Niño events, respectively, indicating false (or opposite) alarms. These results suggest that relationships between PMM and ENSO are highly dependent on the pattern of the PMM.

Figure 3 shows the NDJ SST and 850 hPa wind anomalies corresponding to positive and negative PMM events for two clusters. As expected from Table S1, the central-eastern Pacific is covered by strong SST anomalies with prevailing westerly anomalies during the positive phase of WPMM. The positive SST and westerly wind anomalies gradually developed from the CP with strong off-equatorial signals during the developing phase (Fig. S3a). However, EPMM events do not show any significant SST anomalies in the following winter (Fig. 3c and 3d), since strong negative SST anomalies exist during May-June-July (Fig. S3c). Similarly, negative WPMM events are followed by negative SST anomalies in the central and eastern Pacific with easterly anomalies (Fig. S3b). It is also found that SST anomalies are more significant in the equatorial CP. Yu and Fang (2018) previously suggested that PMM events are more closely related to the development of CP SST anomalies than eastern Pacific SST anomalies, however, EPMM events do not show a strong signal in the equatorial CP.

The strong linkage of WPMM to ENSO development can be explained by its pattern in the equatorial western Pacific. As shown in Figure 3a, strong westerlies prevail in the western Pacific. Since these westerlies are accompanied by positive equatorial CP SSTs, they can persist and be intensified *via* strong air-sea interactions. The western Pacific westerlies induce downwelling Kelvin waves, which play a role in recharging heat content in the central and eastern Pacific (Kug et al. 2010). In addition, these low-frequency westerly anomalies provide a preferable condition for easterly vertical shear of strong westerly wind events (Kug et al., 2009, 2010; Sooraj et al., 2009), a typical pattern of El Niño onset. Therefore, they evolve into a typical El Niño pattern in the following summer and develop further until the end of the calendar year (Fig. 3). However, positive SST anomalies resulting from the positive EPMM are confined to the off-equatorial Pacific (Fig. 2d), which cannot trigger coupled equatorial patterns such as equatorial westerlies and positive CP SST anomaly (Fig. 3c). Without the equatorial western Pacific signals, El Niño tends not to develop. In addition, the prevailing negative SST anomalies and their associated easterlies in the eastern Pacific may play a counteracting role in El Niño development. Consequently, EPMM events are significantly related to El Niño development.

It is well known that the PMM is a useful predictor for ENSO, but PMM events are not always followed by ENSO development, suggesting the existence of some false alarms. Thus far, we showed that there is a preferable pattern of PMM for ENSO development. Our finding suggests that false alarms from PMM information can be reduced if we considered the pattern diversity of the PMM. Following previous methods (Kug et al., 2007; Zhu et al., 2015), we attempted to reconstruct the PMM index based on the two types of spatial SST patterns and comparison with the original PMM index. These new PMM indices depending on PMM diversity are calculated by projecting the C1 and C2 SST patterns shown in Figure 2 into SST anomalies each year (FMAM), and refer to WPMM and EPMM indices, respectively. The correlation coefficient between the ENSO indices and the original PMM index is 0.28 (Fig. 4a); although this is significant, it is difficult to use for prediction. Out of the 33 PMM events defined based on the original PMM events, 13 cases resulted in ENSO development while another 6 PMM events (3 positive and 3 negative cases) were followed by the opposite phases of ENSO. Furthermore, the last 14 PMM events were not linked to ENSO events. Using WPMM events, the correlation increases significantly, reaching 0.64 between the WPMM and ENSO indices (Fig. 4b). We found that WPMM captures 17 ENSO events among the 27 studied WPMM events (14 positive and 13 negative cases) based on 0.7 standard deviation. In detail, 71.4% of positive WPMM events (10 cases) eventually induce El Niño and 53.8% of negative PMM events (7 cases) lead to

La Niña, indicating that the hit rate is 63% on average, which is higher than the 39.4% based on the original PMM index. Moreover, WPMM contains only 2 false alarms among the 27 events, which is an improvement relative to the 6 false alarms in the original PMM events. Furthermore, we also reconstructed the PMM index based on C2 SST patterns, finding that the correlation between EPMM and ENSO is -0.22 (Fig. 4c). This indicates that EPMM cannot be used for ENSO prediction.

4 Conclusion and Discussion

Most previous studies have emphasized that the PMM has a crucial role in triggering ENSO events, however, it has seldom been noticed that the PMM is diverse. This diversity may contribute to its variable impacts on ENSO. Based on the SST patterns, an objective clustering method was used to classify PMM events. We found that PMM cases can be separated into two groups. The WPMM is characterized by a dipole SST anomaly over the west part of ENP whereas the EPMM dominates the CT and coastal SST anomalies in the ENP. Moreover, we showed that approximately 60% of C1 PMM events (5 positive and 4 negative events among 15 C1 PMM cases) are significantly linked to ENSO events, while C2 PMM events are less notably related to ENSO. To utilize our findings for ENSO prediction, we reconstructed WPMM and EPMM indices and found that the WPMM index can accurately predict ENSO events with the higher hit rate (63%) and with fewer false alarm than the original PMM index. The EPMM index constructed based on C2 PMM SST patterns showed an insignificant negative relationship with ENSO, implying that the EPMM SST pattern is not a good predictive framework for ENSO events and requires further investigation.

Although we showed the PMM diversity and its distinct impacts on ENSO, it is not clear what induced this diversity. Previous studies have documented that the NPO has different spatial structures and that an eastward shift of the NPO may favor ENSO occurrence in the following year while the classic NPO pattern with an elongated southern lobe is less related to ENSO occurrence (Park et al. 2013; Sung et al., 2019; Yeh et al., 2018). We also found that the NDJ SLP patterns preceding FMAM PMM are considerably different (Fig. S4). Clearly, WPMM events are related to strong NPO events with a significant eastward shift (Fig. S4a and S4b), consistent with Park et al (2013) and Yeh et al (2018). However, unlike previous studies, we found that EPMM events are less linked to NPO events (Fig. S4c and S4d). Negative EPMM events are associated with significantly negative SLP anomalies over North America but weak positive anomalies south of 40ºN (Fig. S4d). In addition to the impact of NPO, it is also possible that PMM diversity may be connected with SST variability in other basins. For example, some studies have emphasized that the tropical Atlantic SST can modulate off-equatorial SST and wind variabilities along the Pacific ITCZ (Ham et al., 2013; Ham & Kug, 2015; Park et al., 2018; 2019a,b), where the action center of the PMM is located. Moreover, previous studies also found the decadal variation of the PMM is related to the Pacific Decadal Oscillation (PDO; Newman et al., 2016). In this study, however, the decadal variability of the PMM was screened out before the analyses. The mechanism responsible for PMM diversity and its relationship with decadal modes should be a focus of future research.

Acknowledgments:

This work has been funded by the Korea Meteorological Administration Research and Development Program under Grant KMIPA 2018-03212 and the National Research Foundation of Korea (NRF-2018R1A5A1024958). The ERSSTv5 monthly data is downloaded from https://www.esrl.noaa.gov/psd/data/gridded/data.noaa.ersst.v5.html. The NCEP/NCAR reanalysis version I (v1) data is from https://www.esrl.noaa.gov/psd/data/gridded/data.ncep.reanalysis.pressure.html. The PMM index is got from http://www.aos.wisc.edu/~dvimont/MModes/RealTime/PMM.RAW.txt.

References

Amaya, D. J. (2019). The Pacific Meridional Mode and ENSO: a Review. *Current Climate Change Reports*, *5*(4), 296–307. https://doi.org/10.1007/s40641-019-00142-x

Anderson, B. T. (2003). Tropical Pacific sea-surface temperatures and preceding sea level pressure anomalies in the subtropical North Pacific. *Journal of Geophysical Research*, *108*(D23), 4732. https://doi.org/10.1029/2003JD003805

Anderson, B. T. (2007). On the joint role of subtropical atmospheric variability and equatorial subsurface heat content anomalies in initiating the onset of ENSO events. *Journal of Climate*, *20*(8), 1593–1599. https://doi.org/10.1175/JCLI4075.1

Ashok, K., Behera, S. K., Rao, S. A., Weng, H., & Yamagata, T. (2007). El Niño Modoki and its possible teleconnection. *Journal of Geophysical Research*, *112*(C11). https://doi.org/10.1029/2006JC003798

Chang, P., Zhang, L., Saravanan, R., Vimont, D. J., Chiang, J. C. H., Ji, L., et al. (2007). Pacific meridional mode and El Niño-Southern Oscillation. *Geophysical Research Letters*, *34*(16). https://doi.org/10.1029/2007GL030302

Chiang, J. C. H., & Vimont, D. J. (2004). Analogous Pacific and Atlantic Meridional Modes of tropical atmosphere–ocean variability. *Journal of Climate*, *17*(21), 4143–4158. https://doi.org/10.1175/JCLI4953.1

Ham, Y.-G., & Kug, J.-S. (2015). Role of north tropical Atlantic SST on the ENSO simulated using CMIP3 and CMIP5 models. *Climate Dynamics*, *45*(11–12), 3103–3117. https://doi.org/10.1007/s00382-015-2527-z

Ham, Y.-G., Kug, J.-S., Park, J.-Y., & Jin, F.-F. (2013). Sea surface temperature in the north tropical Atlantic as a trigger for El Niño/Southern Oscillation events. *Nature Geoscience*, *6*(2), 112–116. https://doi.org/10.1038/ngeo1686

Huang, B., Thorne, P. W., Banzon, V. F., Boyer, T., Chepurin, G., Lawrimore, J. H., et al. (2017). Extended reconstructed sea surface temperature, Version 5 (ERSSTv5): Upgrades, validations, and intercomparisons. *Journal of Climate*, *30*(20), 8179–8205. https://doi.org/10.1175/JCLI-D-16-0836.1

Kalnay, E., Kanamitsu, M., Kistler, R., Collins, W., Deaven, D., Gandin, L., et al. (1996). The NCEP/NCAR 40-year reanalysis project. *Bulletin of the American Meteorological Society*, *77*(3), 437–471. https://doi.org/10.1175/1520-0477(1996)077<0437:TNYRP>2.0.CO;2

Kao, H.-Y., & Yu, J.-Y. (2009). Contrasting Eastern-Pacific and Central-Pacific Types of ENSO. *Journal of Climate*, *22*(3), 615–632. https://doi.org/10.1175/2008JCLI2309.1

Kaufman, L., & Rousseeuw, P. J. (2009). *Finding groups in data: An introduction to cluster analysis*. New York, NY: John Wiley & Sons. Retrieved from http://nbn-resolving.de/urn:nbn:de:101:1-2014122810037

Kug, J.-S., Jin, F.-F., & An, S.-I. (2009). Two types of El Niño events: Cold tongue El Niño and warm pool El Niño. *Journal of Climate*, *22*(6), 1499–1515. https://doi.org/10.1175/2008JCLI2624.1

Kug, J.-S., Sooraj, K.-P., Li, T., & Jin, F.-F. (2010). Precursors of the El Niño/La Niña onset and their interrelationship. *Journal of Geophysical Research*, *115*(D5), D05106. https://doi.org/10.1029/2009JD012861

Kug, J.-S., Lee, J.-Y., & Kang, I.-S. (2007). Global sea surface temperature prediction using a multimodel ensemble. *Monthly Weather Review*, *135*(9), 3239–3247. https://doi.org/10.1175/MWR3458.1

Larson, S. M., & Kirtman, B. P. (2014). The Pacific Meridional Mode as an ENSO precursor and predictor in the North American multimodel ensemble. *Journal of Climate*, *27*(18), 7018–7032. https://doi.org/10.1175/JCLI-D-14-00055.1

Liu, C., Zhang, W., Stuecker, M. F., & Jin, F. (2019). Pacific Meridional Mode-Western North Pacific tropical cyclone linkage explained by tropical Pacific quasi-decadal variability. Geophysical Research Letters, 46(22), 13346–13354. https://doi.org/10.1029/2019GL085340

Newman, M., Alexander, M. A., Ault, T. R., Cobb, K. M., Deser, C., Di Lorenzo, E., et al. (2016). The Pacific Decadal Oscillation, revisited. *Journal of Climate*, *29*(12), 4399–4427. https://doi.org/10.1175/JCLI-D-15-0508.1

Park, J.-H., Kug, J.-S., Li, T., & Behera, S. K. (2018). Predicting El Niño beyond 1-year lead: Effect of the Western Hemisphere Warm Pool. *Scientific Reports*, *8*(1), 14957. https://doi.org/10.1038/s41598-018-33191-7

Park, J.-H., Li, T., Yeh, S.-W., & Kim, H. (2019a). Effect of recent Atlantic warming in strengthening Atlantic–Pacific teleconnection on interannual timescale via enhanced connection with the Pacific Meridional Mode. *Climate Dynamics*, *53*(1–2), 371–387. https://doi.org/10.1007/s00382-018-4591-7

Park, J.-H., Kug, J.-S., An, S.-I., & Li, T. (2019b). Role of the western hemisphere warm pool in climate variability over the western North Pacific. *Climate Dynamics*. https://doi.org/10.1007/s00382-019-04652-0

Park, J.-Y., Yeh, S.-W., Kug, J.-S., & Yoon, J. (2013). Favorable connections between seasonal footprinting mechanism and El Niño. *Climate Dynamics*, *40*(5–6), 1169–1181. https://doi.org/10.1007/s00382-012-1477-y

Rogers, J. C. (1981). The North Pacific Oscillation. *Journal of Climatology*, *1*(1), 39–57. https://doi.org/10.1002/joc.3370010106

Sooraj, K. P., Kim, D., Kug, J.-S., Yeh, S.-W., Jin, F.-F., & Kang, I.-S. (2009). Effects of the low-frequency zonal wind variation on the high frequency atmospheric variability over the tropics. *Climate Dynamics*, *33*(4), 495–507. https://doi.org/10.1007/s00382-008-0483-6

Stuecker, M. F. (2018). Revisiting the Pacific Meridional Mode. *Scientific Reports*, *8*(1), 3216. https://doi.org/10.1038/s41598-018-21537-0

Sung, M.-K., Jang, H.-Y., Kim, B.-M., Yeh, S.-W., Choi, Y.-S., & Yoo, C. (2019). Tropical influence on the North Pacific Oscillation drives winter extremes in North America. *Nature Climate Change*, *9*(5), 413–418. https://doi.org/10.1038/s41558-019-0461-5

Vimont, D. J., Battisti, D. S., & Hirst, A. C. (2001). Footprinting: A seasonal connection between the tropics and mid-latitudes. *Geophysical Research Letters*, *28*(20), 3923–3926. https://doi.org/10.1029/2001GL013435

Vimont, D. J., Wallace, J. M., & Battisti, D. S. (2003). The seasonal footprinting mechanism in the Pacific: Implications for ENSO. *Journal of Climate*, *16*(16), 2653–2667.

Wang, B., Luo, X., Yang, Y.-M., Sun, W., Cane, M. A., Cai, W., et al. (2019a). Historical change of El Niño properties sheds light on future changes of extreme El Niño. *Proceedings of the National Academy of Sciences*, *116*(45), 22512–22517. https://doi.org/10.1073/pnas.1911130116

Wang, B., Chen, G., & Liu, F. (2019b). Diversity of the Madden-Julian Oscillation. *Science Advances*, *5*(7), eaax0220. https://doi.org/10.1126/sciadv.aax0220

Wilks, D. S. (2011). *Statistical Methods in the Atmospheric Sciences*.

Xie, S.-P., & Philander, S. G. H. (1994). A coupled ocean-atmosphere model of relevance to the ITCZ in the eastern Pacific. *Tellus A: Dynamic Meteorology and Oceanography*, *46*(4), 340–350. https://doi.org/10.3402/tellusa.v46i4.15484

Yang, S., Li, Z., Yu, J.-Y., Hu, X., Dong, W., & He, S. (2018). El Niño–Southern Oscillation and its impact in the changing climate. *National Science Review*, *5*(6), 840–857. https://doi.org/10.1093/nsr/nwy046

Yeh, S.-W., Kug, J.-S., Dewitte, B., Kwon, M.-H., Kirtman, B. P., & Jin, F.-F. (2009). El Niño in a changing climate. *Nature*, *461*(7263), 511–514. https://doi.org/10.1038/nature08316

Yeh, S.-W., Yi, D.-W., Sung, M.-K., & Kim, Y. H. (2018). An eastward shift of the North Pacific Oscillation after the mid-1990s and its relationship with ENSO. *Geophysical Research Letters*, *45*(13), 6654–6660. https://doi.org/10.1029/2018GL078671

Yu, J.-Y., & Fang, S.-W. (2018). The distinct contributions of the seasonal footprinting and charged-discharged mechanisms to ENSO complexity. *Geophysical Research Letters*, *45*(13), 6611–6618. https://doi.org/10.1029/2018GL077664

Yu, J.-Y., & Kim, S. T. (2011). Relationships between extratropical sea level pressure variations and the Central Pacific and Eastern Pacific types of ENSO. *Journal of Climate*, *24*(3), 708–720. https://doi.org/10.1175/2010JCLI3688.1

Yu, J.-Y., Kao, H.-Y., & Lee, T. (2010). Subtropics-related interannual sea surface temperature variability in the Central Equatorial Pacific. *Journal of Climate*, *23*(11), 2869–2884. https://doi.org/10.1175/2010JCLI3171.1

Yu, J.-Y., Wang, X., Yang, S., Paek, H., & Chen, M. (2017). The changing El Niño-Southern Oscillation and associated climate extremes. In S.-Y. S. Wang, J.-H. Yoon, C. C. Funk, &

R. R. Gillies (Eds.), *Geophysical Monograph Series* (pp. 1–38). Hoboken, NJ, USA: John Wiley & Sons, Inc. https://doi.org/10.1002/9781119068020.ch1

Zhu, Z., Li, T., Hsu, P., & He, J. (2015). A spatial–temporal projection model for extended-range forecast in the tropics. Climate Dynamics, 45(3–4), 1085–1098. https://doi.org/10.1007/s00382-014-2353-8

Figures:

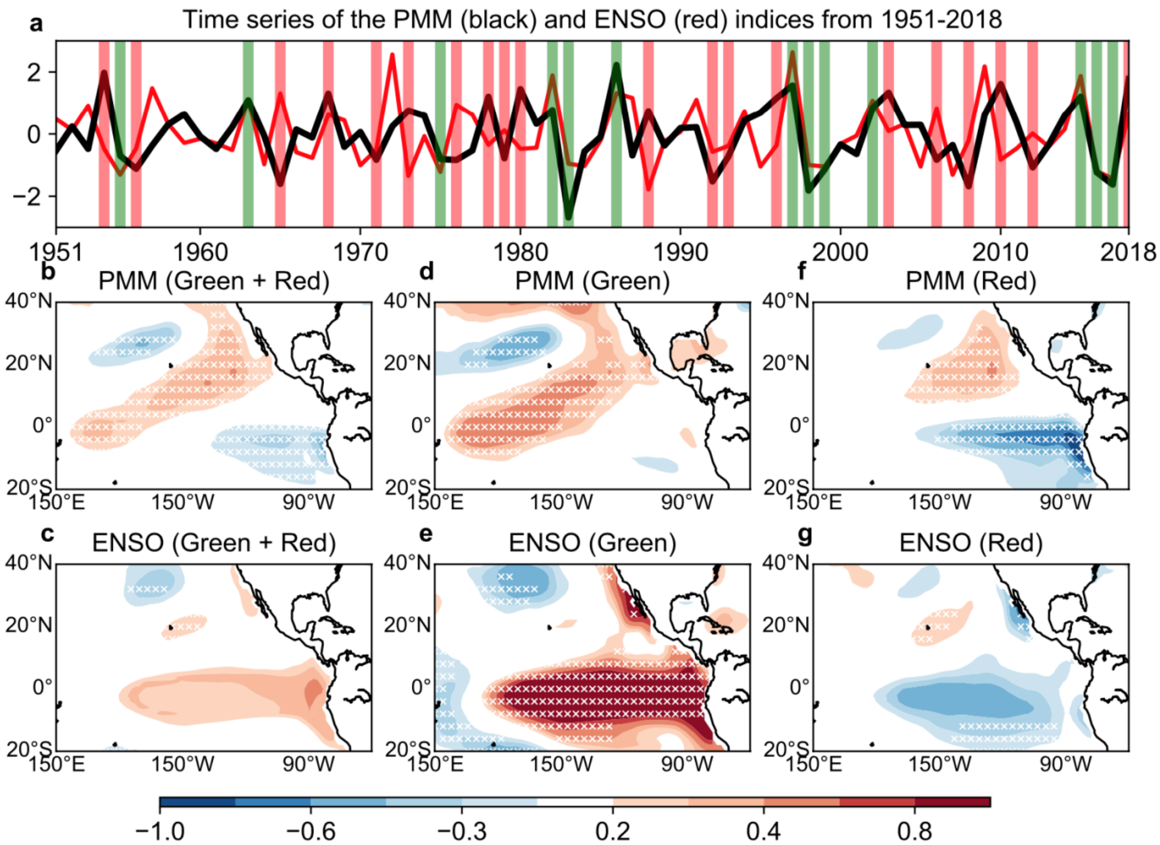

Figure 1. Time series (a) of the PMM and ENSO indices from 1951-2018 and the spring (FMAM; b, d and f) and winter (NDJ; c, e and g) SST anomalies between positive and negative PMM years. (a) Normalized PMM (black line) and following NDJ averaged Niño3.4 (red line) indices for the period 1951-2018. Green and red bars indicate PMM events larger than ±0.7 standard deviation. Green bars represent the 13 (6 positive and 7 negative) PMM events associated with ENSO occurrence while red bars represent the other 20 (10 positive and 10 negative) PMM events (i.e., a total of 33 PMM events). (b) the composite of SST anomalies from 16 positive and 17 negative PMM events; (c) corresponding NDJ SST anomalies based on 33 PMM events; (d) composite of SST anomalies of 13 PMM events shown as green bars; (e) composite of NDJ SST anomalies based on the 13 PMM years represented by green bars; (f) same as (d) but for the 20 PMM events indicated by red bars; (g) same as (e) but for the 20 PMM years shown as red bars. White crosses represent areas of SST above 95% significance level.

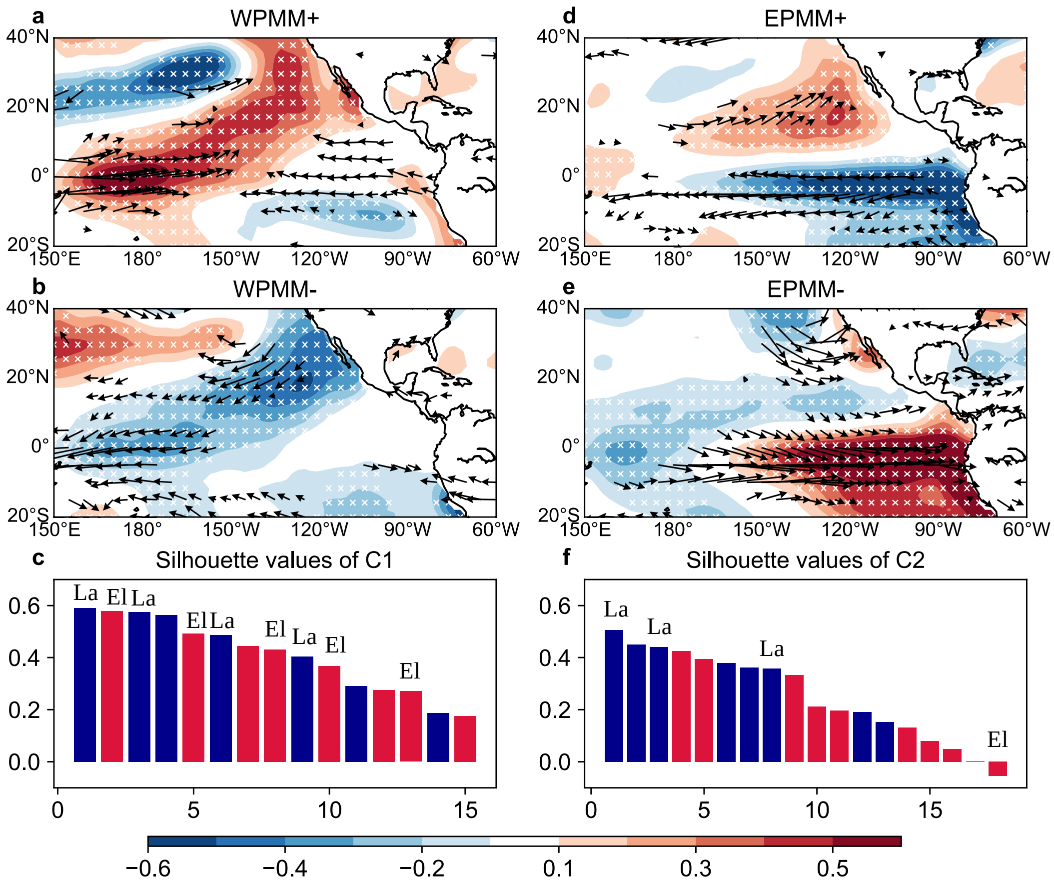

Figure 2. Two clusters of PMM events and silhouette values of each event. Cluster 1 (C1; left panel) (a) positive and (b) negative PMM events; cluster 2 (C2; right panel) (c) positive and (d) negative PMM events; silhouette values for (e) C1 and (f) C2 PMM events. White crosses in a, b, d and e represent areas of anomalous SST fields above 90% confidence level based on a two-tailed t test; black arrows indicate the composite of 850 hPa winds (m/s) above 90% confidence level. Red (blue) bars in (c) and (f) represent the positive (negative) PMM events, respectively. “El” and “La” marked above the bars in (c) and (f) indicate that El Niño or La Niña events occurred during the respective positive and negative PMM phases.

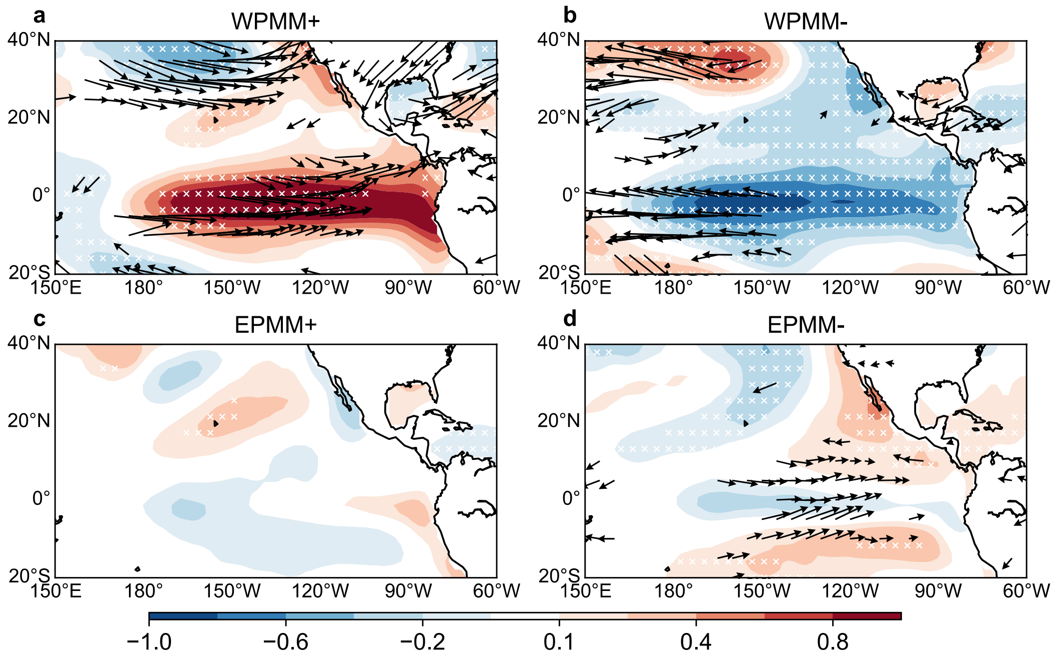

Figure 3. Composites of NDJ averaged SST anomalies and wind anomalies at 850hPa based on different types of PMM years. (a) Composite NDJ SST anomalies during C1 positive PMM years; (b) same as (a) but for C1 negative PMM years; (c) same as (a) but for C2 positive PMM years; and (d) same as (b) but for negative C2 PMM years. White crosses and black arrows indicate area above 90% confidence level.

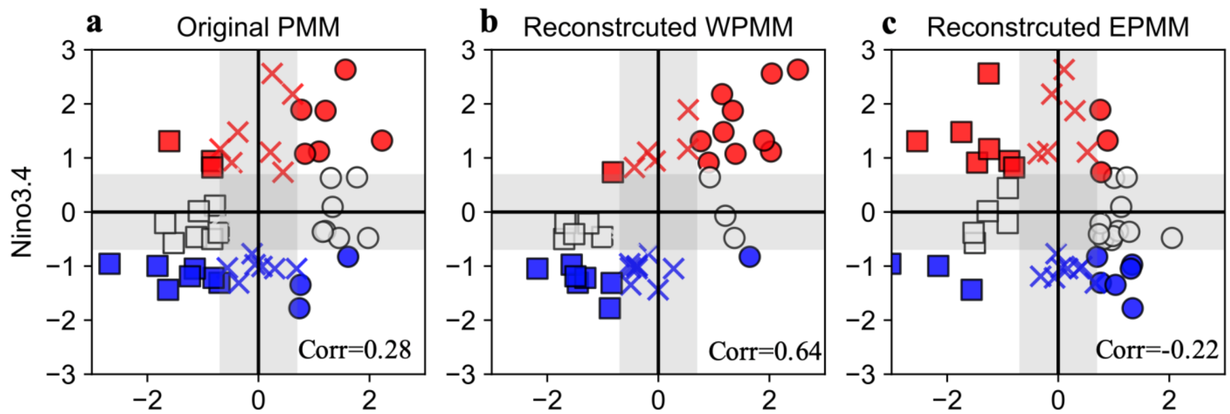

Figure 4. Scatter diagrams of ENSO index and original (reconstructed) PMM index based on C1 and C2 spatial patterns for the period 1951-2018. (a) Scatter plot of ENSO and original PMM indices; (b) scatter plot of ENSO index and WPMM index reconstructed based on the C1 SST pattern; and (c) scatter plot of ENSO index and EPMM index reconstructed based on the C2 SST pattern. Significant El Niño and La Niña events are colored red and blue, respectively. Significant positive and negative PMM events are marked by circles and rectangles, respectively.

AGU PUBLICATIONS

Geophysical Research Letters

Supporting Information for

Diversity of Pacific Meridional Mode and its distinct impacts on El Niño-Southern Oscillation

Jiuwei Zhao[1], Jong-Seong Kug[1,2*], Jae-Heung Park[1] and Song-Il An[2]

1. Division of Environmental Science and Engineering, Pohang University of Science & Technology (POSTECH), Pohang, Korea
2. I_CREATE / Institute for Convergence Research and Education in Advanced Technology, Yonsei Univeristy, Seoul, Korea
3. Department of Atmospheric Sciences, Yonsei Univeristy, Seoul, Korea

*Corresponding author: Prof. Jong-Seong Kug

Division of Environmental Science and Engineering (DESE),

Pohang University of Science and Technology (POSTECH), Korea.

Email: jskug1@gmail.com

Contents of this file

Table S1. Positive and negative PMM (WPMM and WPMM) events chosen based on the criterion of ±0.7 standard deviation. Red represents El Niño years; blue denotes La Niña years.

	Positive	Negative
WPMM	**1963**, 1980, **1986, 1997**, **2002**, 2010, **2015**	**1955**, 1956, 1971, **1975**, 1979, **1999**, 2008, **2016**
EPMM	1954, 1968, **1973**, 1978, **1982**, **1988**, 1996, 2003, 2018	**1965**, **1976**, **1983**, 1992, 1993, **1998**, **2006**, 2012, **2017**

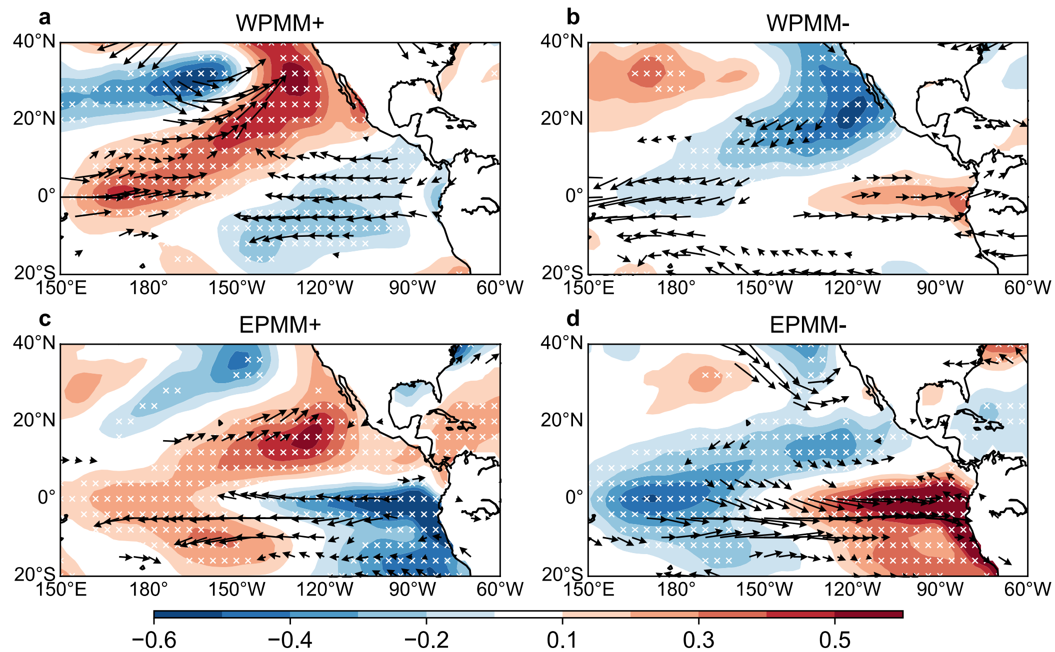

Figure. S1. Clustering analysis with simultaneous El Niño signal removed. The cluster 1 (C1) (a) positive and (b) negative western PMM (WPMM) events; and cluster 2 (C2) (c) positive and (d) negative eastern PMM (EPMM) events. The white crosses represent composite of SST (℃) with area above 90% confidence level based on two-tailed t test and the black arrows indicate the composite of 850hPa winds (m/s) above 90% confidence level.

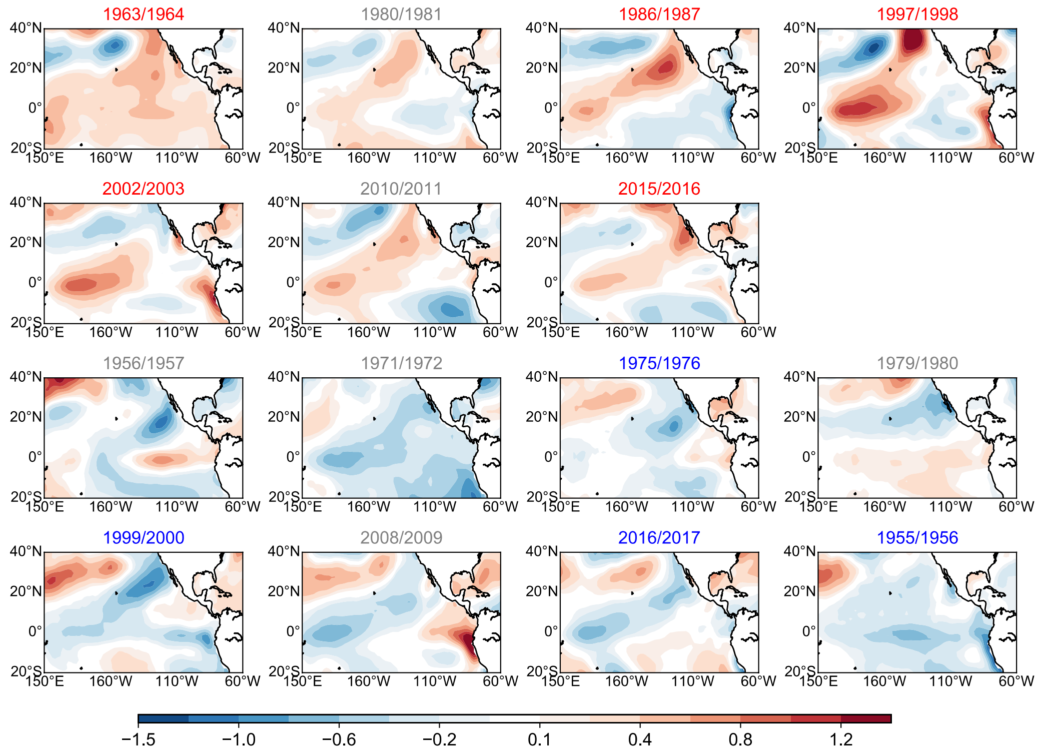

Figure S2. The spring SST anomalies of 15 individual C1 PMM events. The year marked by red (blue) color represents the El Niño (La Niña) year, respectively.

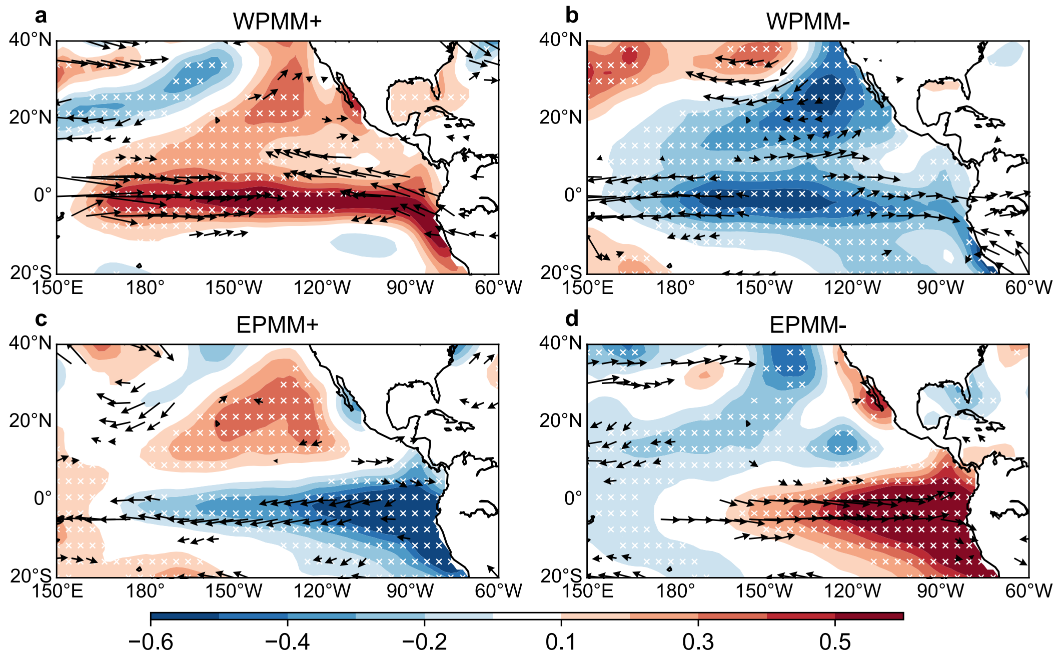

Figure S3. Composites of May-June-July (MJJ) averaged SST and 850hPa wind anomalies based on different types of PMM years. (a) The composite MJJ SST anomalies during positive WPMM years; (b) same as (a) but for negative WPMM years; (c) the composite MJJ SST anomalies during positive EPMM years; and (d) same as (c) but for negative EPMM years. The white crosses represent area above 90% confidence level based on Student's and the black arrows indicate the composite of 850hPa winds (m/s) above 90% confidence level.

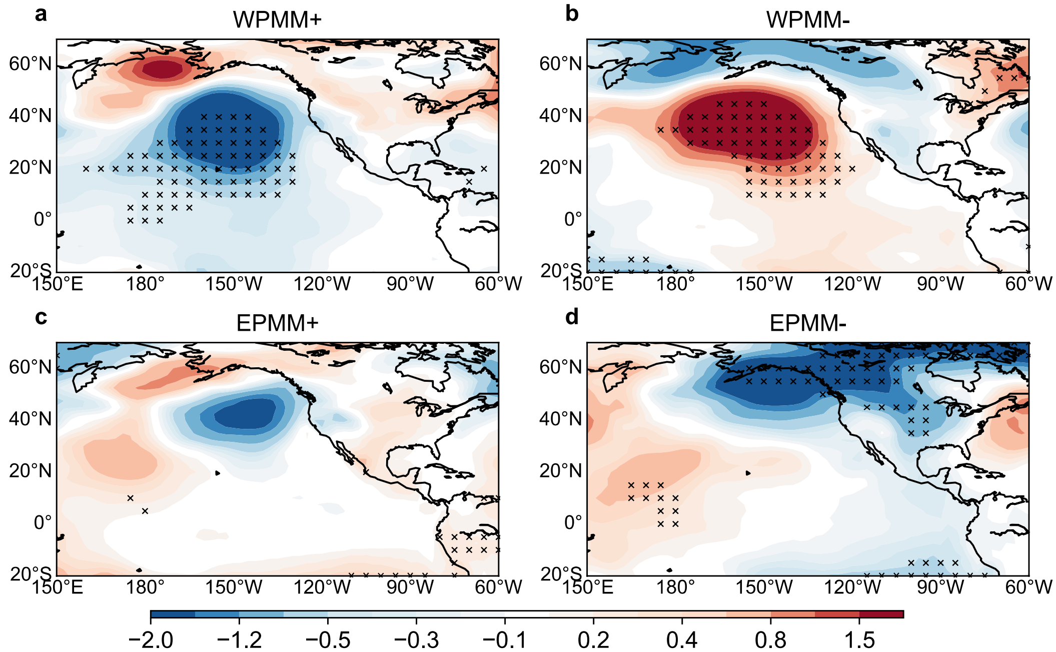

Figure S4. The composite of previous NDJ SLP anomaly based on FMAM PMM events for the period 1950-2018. (a) the NDJ SLP anomalies based on C1 positive PMM events; (b) same as (a) but for C1 negative PMM cases; (c) same as (a) but for C2 positive PMM years; (d) same as (b) but for C2 negative PMM years.